PHAS0054 PRACTICAL PHYSICS 3

Computational Methods for Investigating Series RLC, RC and RC-CR Circuits

Introduction

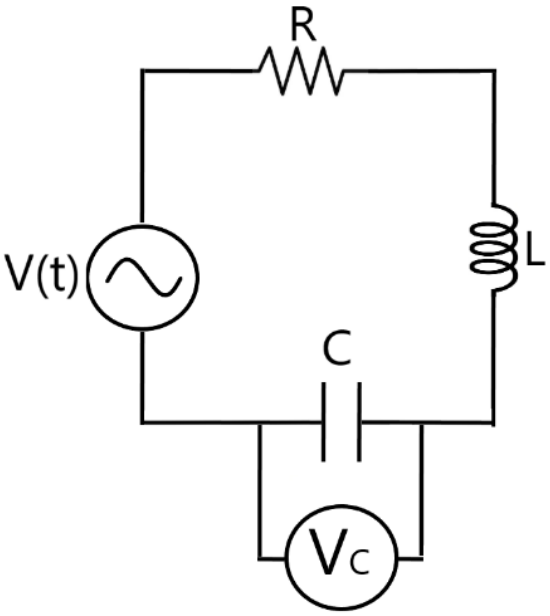

Figure 1 : Schematic illustration of an RLC Circuit with component values R, L, C, AC input voltage V(t) and capacitor voltage Vc

According to Kirchoff's laws the sum of the voltages around a series circuit equals zero.

For the RLC circuit shown in figure 1, this results in equation 1.

$$V(t) = L\ddot{Q} + \dot{Q}R + QC^{-1} \qquad (1)$$

This system is an example of a damped harmonic oscillator, where the damping is provided by the resistance R. The system shows the phenomenon of resonance which occurs when the driving frequency, here provided by the AC input V(t) matches some natural frequency of the system. At resonance, maximum amplitude is achieved[1], here measured as the capacitor voltage V_C. When an inductor and capacitor are placed in series, a bandpass circuit emerges where low frequencies are impeded by the inductor and high frequencies are impeded by the capacitor, resulting in a middle band of frequencies being put through, the amplitude of which depends on the resistance R.

The measured amplitude V_C tapers off as the driving frequency is changed around the resonance or natural frequency. In this way, the RLC circuit acts both as a bandpass filter where it dampens the amplitude of frequencies both below and above the resonant frequency and an amplifier, for small R, at the resonant frequency.

If the inductance L is made 0, the series RC circuit can be modelled as shown in figure 2.

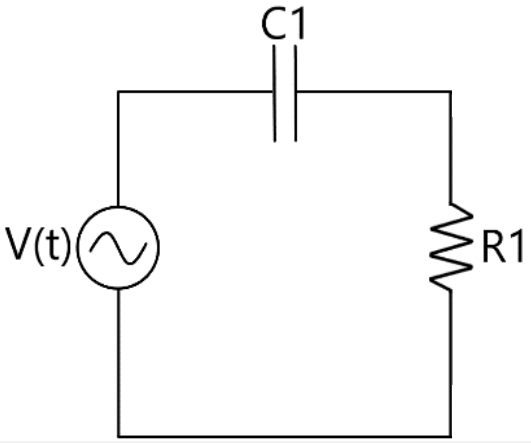

Figure 2 : Schematic illustration of a series RC circuit with component values R1, C1 and AC input voltage V(t)

Where the resultant ODE, using Kirchhoff's Laws, is shown in equation 2.

$$V(t) = \dot{Q}R_1 + QC_1^{-1} \qquad (2)$$

The capacitor acts as a low pass filter while the resistor acts as a high pass filter. So, a voltage read at V_{C1} will peak at low frequencies while a voltage at V_{R1} will peak at high frequencies.

If two such RC circuits are placed in series themselves, we obtain a RC-CR bandpass filter shown in figure 3.

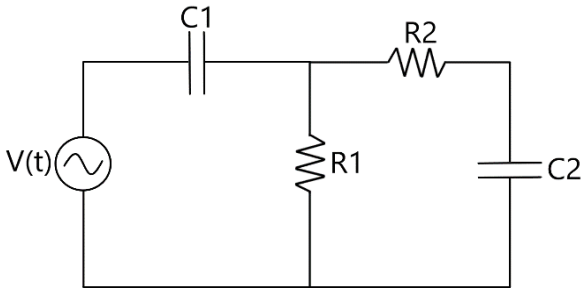

Figure 3 : Schematic illustration of RC-CR circuit

Where the voltage measured at C2 peaks in some middle band of frequencies that is between some cut-off frequencies f_1 and f_2. The cut-off frequency f_C is defined in equation 3, where the peak voltage is reduced by -3dB.

$$f_C = \frac{1}{2\pi RC} \qquad (3)$$

By adjusting the R and C values, a variety of narrow-band, wide-band and band-stop filters can be constructed.

Here, we use Matlab to solve the ODEs for the RLC, RC and RC-CR systems numerically and compare the results with experimental data.

Methodology

Matlab provides an ode solver function ode45[2] shown in equation 4.

$$[t, y] = \text{ode45}(\text{ode}, \text{tspan}, y0) \qquad (4)$$

Ode45 integrates the provided ode function within the limits in tspan for some initial conditions y0.

All Matlab ode solver functions, however, can only solve 1st order ODEs. To solve our second order ODE for the RLC system, the substitution in equation 5

$$\dot{Q}_1 = Q_2 \qquad (5)$$

$$\dot{Q}_2 = \frac{V(t) - RQ_2 - C^{-1}Q_1}{L} \qquad (6)$$

decomposes our 2nd order ODE, in equation 1, into two coupled 1st order ODEs, equations 5 and 6, which are then put into the ode45 function.

The solutions are then our charge Q_1 and current Q_2 against time t.

By varying V(t) i.e. changing the frequency and component values R, L and C, the behaviour of V_C can be studied for different frequencies and component values. In this investigation, the behaviour of V_C was studied against a range of frequencies for different R values.

To solve the series RC circuit, equation 2 can be input directly into ode45 to be solved over a range of frequencies, where the voltages at C1 and R1 are obtained using the relationships in equation 2.

The RC-CR bandpass system is solved in two steps. Ode45 is used to solve the voltage equation for the first loop of components, the ODE for which, as before, is equation 2.

The resultant peak voltages V_{R1} at each frequency f are used as input voltage for the second loop of components, the ODE for which is shown in equation 7.

$$V_{R1} = \dot{Q}R_2 + QC_2^{-1} \qquad (7)$$

Where V(t) has been replaced with V_{R1}. The voltage measured at C2 then gives rise to a bandpass filter where both low and high frequencies are greatly impeded but mid-level frequencies are put through.

Results and Discussion

The RLC model was looped across a range of frequencies from f = 10,000 Hz to f = 100,000 Hz, for a low damping resistance LDR = 853 Ω and a high damping resistance HDR = 1530 Ω.

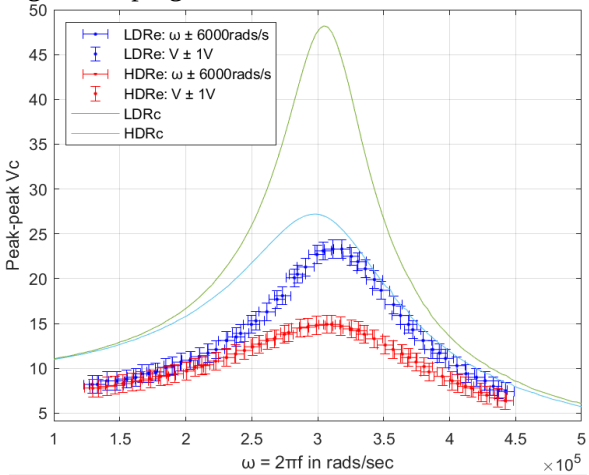

Figure 4: Experimental and Computational response of V_C against driving frequency where the experimental low damping resistance LDR_E and high damping resistance HDR_E data is shown in blue and red and the computational low damping resistance LDR_C and high damping resistance HDR_C in green and blue, respectively

Figure 4 shows an overlay of the experimental, subscript e, and computational, subscript c, data. The experimental data is represented via vertical (experimental errors in voltage) and horizontal (experimental errors in frequency) error bars.

Three observations can be made immediately. The modelled data shows (i) Higher peak amplitudes for both low and high damping resistors, (ii) a shift to the left compared to the experimental data i.e. resonant frequencies are lower for the modelled data and (iii) sharper peaks with higher Q-factors. Data presented in table 1 provides further confidence in these cursory observations, where LDR_M = 853 Ω, HDR_M = 1530 Ω, LDR_E = 853 ± 7 Ω and HDR_E = 1530 ± 10 Ω, the M stands for modelled and the E for experimental.

When the circuit is first switched on the system goes through a transient stage before the oscillations become regular and we achieve steady state oscillations. For our computational model, this means that the first few waveforms will result in erroneous data if used in peak-peak V_C calculations. For this reason, only data after n/2 oscillations, where n is the total number of oscillations over time tspan, was used for all calculations.

The behaviour of the modelled circuits can be understood if properties of the capacitor and inductor are considered[3]. The voltage at the inductor V_L and capacitor V_C is given by equations 8 and 9, respectively.

$$V_L = \frac{X_L}{\sqrt{R^2+(X_L-X_C)^2}}V(t) \qquad (8)$$

$$V_C = \frac{X_C}{\sqrt{R^2+(X_L-X_C)^2}}V(t) \qquad (9)$$

Where the inductive and capacitive reactance is given by equations 10 and 11, respectively.

$$X_L = 2\pi fL \qquad (10)$$

$$X_C = \frac{1}{2\pi fC} \qquad (11)$$

So, as driving frequency f increases the inductive reactance X_L increases, leading to an increase in the output voltage V_L. Therefore, an inductor acts as a high-pass filter where low frequencies are heavily impeded. Similarly, high frequencies result in low capacitive reactance and therefore the capacitor acts as a low pass filter, where high frequencies are greatly impeded.

No real-life circuit has zero resistance everywhere except for at the resistor. The wires themselves introduce a resistance, along with the other components, namely the inductor and capacitor, also contribute to the total resistance. This extra resistance R_+ is unaccounted for by the computational model.

	R	V_{peak} (V)	ω_{peak} (rads/s)	Q
M	LDR_M	48.2	304734	4.7
	HDR_M	27.3	298451	2.5
E	LDR_E	23.3	305024	3.1 ± 0.2
	HDR_E	14.9	297572	1.9 ± 0.2

Table 1 : Summary of findings from modelled M and experimental E data for the RLC model

The modelled data shows resonant frequencies that are lower than the experimental data. Looking at the mathematically calculated peak frequency ω[1] of an RLC circuit given in equation 12

$$\omega^2 = \frac{1}{\frac{L}{C}} - \frac{R^2}{2L^2} \qquad (12)$$

We see that an increase in the resistance R lowers the resonant frequency ω, thereby shifting a resonance response curve to the left. However, since we know that the model is underestimating the resistance R, not overestimating it, the modelled data should be shifted to the right compared to the experimental data, not left.

Other factors that contribute to the discrepancy between modelled and experimental data are mutual inductance and parasitic capacitance.

An amended model of the RLC circuit is run where the R, L and C values are manually altered to best match the experimental work. Figure 5 shows the result. A better but not perfect fit is obtained, with the computational data still largely lying outside experimental errors. The component values used in the original RLC computational model (figure 4) and the amended model (figure 5) is summarised in table 2.

	LDR(Ω)	HDR(Ω)	L(mH)	C(pF)
O	853	1530	13.4	785
A	1353	2030	9.38	942

Table 2 : Component values used in the O = original and A = amended RLC computational model

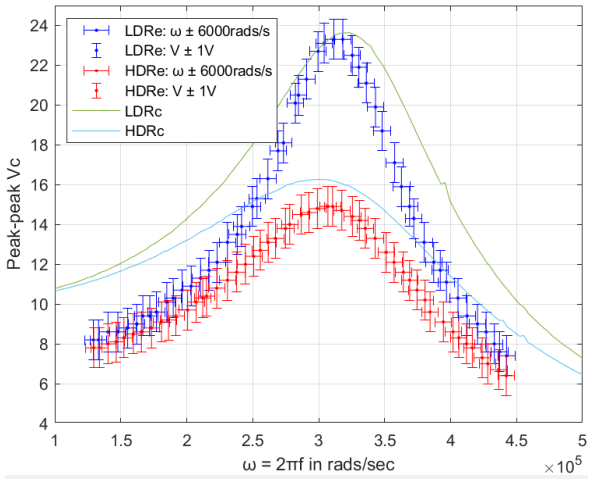

Figure 5 : Experimental and Computational response of V_C against driving frequency using an adjusted RLC model with 500Ω added to the resistance. Inductance has been adjusted by L – 4.02mH and capacitance C + 157pF

In general, increasing R shifts the modelled curve down and to the left while increasing L or C just shifts the curve to the left. It was found that a high enough value of R that matched our experimental results produced modelled data that was far too much to the left, adjustments to the L and C values then gave a better match. These manual adjustments are compared to the theoretically estimated values obtained from equations 13 and 15 later.

Mutual inductance arises here when the high frequency emf produces a rapidly changing magnetic field which induces additional emf in any components nearby. Due to the proximity of the components on a breadboard, mutual inductances can be quite large. Unaccounted for mutual inductances could be the explanation behind why the model is shifted to the left of the experimental data instead of the right. If the experimental circuit has a much higher inductance than the stated inductance L, that would increase the value ω^2 and therefore shift the experimental resonance curve to the right.

An alternative much simpler explanation could be that the value stated on the inductor and capacitor used was not accurate. The components had no stated tolerances so no comparison can be made there.

Mutual inductances[4] in a circular loop can be estimated by equation 13.

$$I = \mu_0 r\left[\ln\left(\frac{8r}{a}\right) - 2 + \frac{1}{4}Y\right] \qquad (13)$$

Where r = Loop Radius, a = Wire Radius, μ_0 = permeability of free space, μ = specific permeability of wire, σ = specific conductivity of wire and Y is given by equation 14.

$$Y \approx \frac{1}{1+a\sqrt{\frac{1}{8}\mu\sigma\omega}} \qquad (14)$$

The mutual inductance was estimated to be ~11mH using r = 0.05m, a = 0.001m, μ = 1.256629×10^{-6} H/m and σ = 5.96×10^{7} S/m of Copper and $\omega = 10^6$ Hz.

Parasitic capacitance arises because charge is stored in the electric field between two electrical components that have a non-zero potential difference in proximity, with larger resistance R producing larger parasitic capacitances. Parasitic capacitance in the experimental circuit could also contribute to higher than expected resonant frequencies, however this is unlikely as a large unaccounted-for capacitance would be needed.

Parasitic capacitance[5] between parallel wires of infinite length above ground can be estimated by equation 15

$$C = \frac{12.031}{\log_{10}\left[\frac{d}{2a}\left(1+\sqrt{1-\frac{1}{\left(\frac{d}{2a}\right)^2}}\right)\right]} \qquad (15)$$

Where a = Wire Radius and d = distance between wires.

The parasitic capacitance was estimated to be ~7pF using d = 0.05m and a = 0.001m.

The agreement between the manually adjusted inductance in the computational model and the estimated mutual inductance obtained from equation 13 is within an order of a magnitude. However, the agreement between adjusted capacitance and the estimated parasitic

capacitance from equation 15 is off by two orders of magnitude.

This suggests that the experimental RLC circuit either has a significant systematic error or that parasitic capacitance is much larger than anticipated.

The RC circuit was looped from f = 5,000 Hz to f = 500,000 Hz, for a LDR = 1000 Ω and a HDR = 10,000 Ω, at a low capacitance of C = 780pF, presented in figure 6, and a higher capacitance of C = 7850pF, presented in figure 7.

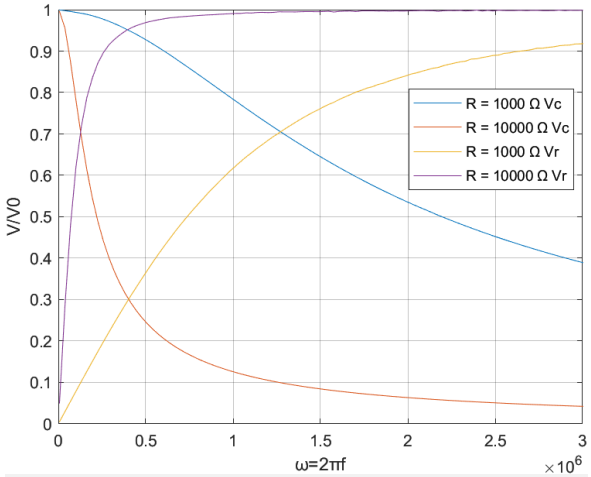

Figure 6 : Voltage gain ($V_{OUT}/V(t)$) of V_C and V_R against driving frequency in a computational series RC circuit with Capacitance = 785pF

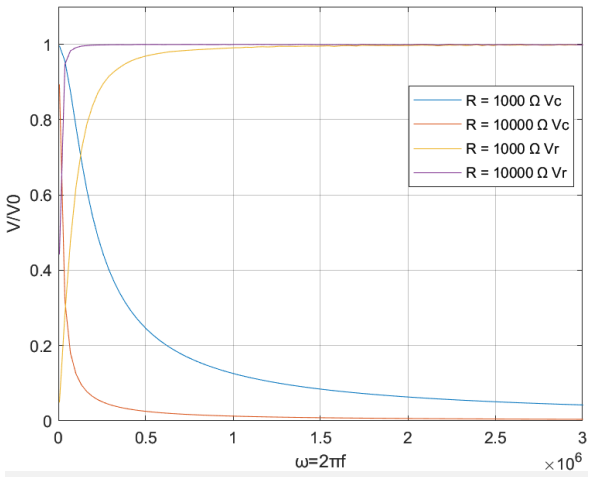

Figure 7 : Voltage gain ($V_{OUT}/V(t)$) of V_C and V_R against driving frequency in a computational series RC circuit with Capacitance = 7850pF

V_C peaks at lower frequencies, where the capacitor acts as a low pass filter, and V_R peaks at higher frequencies, where the resistor acts as a high pass filter. The slope of the response curve is more sensitive to capacitance than resistance, as can be seen from figures 6 and 7 where while a sharper response is observed upon increasing the resistance by an order of a magnitude, an even sharper response is observed upon increasing the capacitance by the same order of magnitude.

This knowledge was used to model the RC-CR bandpass filter which was also looped from f = 5,000 Hz to f = 500,000 Hz with R1 = 2000 Ω, C1 = 4 nF, R2 = 500 Ω and C2 = 8 nF and the results displayed in figure 8. f_{C1} and f_{C2} show the cut-off frequencies, calculated from equation 3. The system was found to be a better low frequency bandpass filter than a high frequency band pass filter. This is apparent from figure 7 and the shape of the response of V_C and V_R, where the RC-CR circuit essentially superimposes the V_R and V_C response observed in the RC circuit.

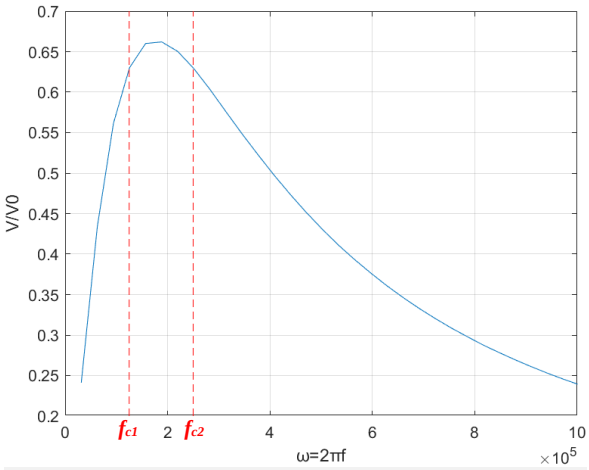

Figure 8 : Voltage gain at C2 in response to driving frequency in a RC-CR circuit

Conclusions and Further Work

Herein, we have demonstrated the use of MATLAB to model a series RLC, RC and RC-CR circuit. Poor agreement is seen between the experimental and modelled RLC circuit. Adjustment to the L, C and R values produces decent but not still not perfect agreement between results. This can be attributed to systematic errors and the use of large voltages introducing significant interference effects, namely parasitic capacitance and mutual inductance.

The RC circuit is seen to act as a low-pass filter, where V_C is measured, and a high-pass filter, where V_R is measured and is observed to be more sensitive to changes in capacitance than to resistance. The circuit acts as a decent bandpass

filter for low frequencies, with sub-optimal gain at resonance. Practical applications would require the use of an amplifier or further modification to the circuit.

Avenues for further work include modifying the MATLAB code so that the model can trial various R, L and C values in a loop that tries to minimise the difference between modelled and experimental data points. This should give more true-to-life R, L, C values than the ones obtained manually here. Further changes can be made to the code so that running the RC-CR circuit is a more seamless process. Should the model be used for predictive purposes, the lossless version developed here should be modified to accept additional data like thickness and length of wires, approximate proximity of components and any emf shielding employed. So that it can approximate mutual inductance, parasitic capacitance and any additional resistances, giving good agreement with some practical RLC, RC or RC-CR circuit.

References

[1] R. Lewis and R. Lewis, "LCR Circuits," in *Electronics Servicing*, Macmillan Education UK, 1983, pp. 1–29.

[2] "Solve nonstiff differential equations — medium order method - MATLAB ode45 - MathWorks United Kingdom." [Online]. Available: https://uk.mathworks.com/help/matlab/ref/ode45.html. [Accessed: 22-Feb-2020].

[3] "Band Pass Filters." [Online]. Available: http://info.ee.surrey.ac.uk/Teaching/Courses/ee1.cct/circuit-theory/section8/bandpass.html. [Accessed: 22-Feb-2020].

[4] "Electromagnetics: History, theory, and applications - University College London." [Online]. Available: https://ucl-new-primo.hosted.exlibrisgroup.com/primo-explore/fulldisplay?docid=TN_scopus2-s2.0-85036582874&context=PC&vid=UCL_VU2&lang=en_US&search_scope=CSCOP_UCL&adaptor=primo_central_multiple_fe&tab=local&query=any,contains,electromagnetics%20history%20theory%20and%20applications,%20elliott%20robert%20stratman&offset=0. [Accessed: 30-Mar-2020].

[5] "Radio engineers' handbook / by Frederick Emmons Terman - University College London." [Online]. Available: https://ucl-new-primo.hosted.exlibrisgroup.com/primo-explore/fulldisplay?docid=UCL_LMS_DS21130934440004761&context=L&vid=UCL_VU2&lang=en_US&search_scope=CSCOP_UCL&adaptor=Local%20Search%20Engine&tab=local&query=any,contains,F.E.%20Terman,%20Radio%20Engineers%27%20Handbook,%20McGraw-Hill,%20New%20York,%201943&offset=0. [Accessed: 30-Mar-2020].